Homer1 mediates CaSR-dependent activation of mTOR complex 2 and initiates a novel pathway for AKT-dependent β-catenin stabilization in osteoblasts

Received for publication, November 7, 2018, and in revised form, August 19, 2019 Published, Papers in Press, September 16, 2019, DOI 10.1074/jbc.RA118.006587

Mark S. Rybchyn[‡], Kazi S. Islam[§], Tara C. Brennan-Speranza[‡], Zhiqiang Cheng[¶], Sarah C. Brennan[§], Wenhan Chang[¶], Rebecca S. Mason[‡1], and Arthur David Conigrave[§2]

From the [‡]Discipline of Physiology, School of Medical Sciences and Bosch Institute, University of Sydney, New South Wales 2006, Australia, the [§]School of Life and Environmental Science, Charles Perkins Centre (D17) and Bosch Institute, University of Sydney, New South Wales 2006, Australia, and the [¶]School of Medicine, University of California, San Francisco, California 94121

Edited by Xiao-Fan Wang

The calcium-sensing receptor (CaSR) is critical for skeletal development, but its mechanism of action in osteoblasts is not well-characterized. In the central nervous system (CNS), Homer scaffolding proteins form signaling complexes with two CaSR-related members of the G protein–coupled receptor (GPCR) family C, metabotropic glutamate receptor 1 (mGluR1) and mGluR5. Here, we show that CaSR and Homer1 are co-expressed in mineralized mouse bone and also co-localize in primary human osteoblasts. Co-immunoprecipitation experiments confirmed that Homer1 associates with CaSR in primary human osteoblasts. The CaSR–Homer1 protein complex, whose formation was increased in response to extracellular Ca^{2+}, was bound to mechanistic target of rapamycin (mTOR) complex 2 (mTORC2), a protein kinase that phosphorylates and activates AKT Ser/Thr kinase (AKT) at Ser^{473}. siRNA-based gene-silencing assays with primary osteoblasts revealed that both CaSR and Homer1 are required for extracellular Ca^{2+}-stimulated AKT phosphorylation and thereby inhibit apoptosis and promote AKT-dependent β-catenin stabilization and cellular differentiation. To confirm the role of the CaSR–Homer1 complex in AKT initiation, we show that in HEK-293 cells, co-transfection with both *Homer1c* and *CaSR*, but neither with *Homer1c* nor *CaSR* alone, establishes sensitivity of AKT–Ser^{473} phosphorylation to increases in extracellular Ca^{2+} concentrations. These findings indicate that Homer1 mediates CaSR-dependent AKT activation via mTORC2 and thereby stabilizes β-catenin in osteoblasts.

CaSR[3] is a family C G-protein–coupled receptor (GPCR) critical for the development of bone and cartilage (1–3) and contributes to the development of the CNS, in part by promoting the differentiation of oligodendrocytes and formation of cerebral white matter (4). When CaSR exon-7, encoding the receptor's heptahelical domain and intracellular C terminus, was selectively knocked out of early osteoblast lineage cells in mice, bone mass was greatly reduced (1, 2), and selective deletion in chondrocytes was embryonic lethal (1). In a human case of neonatal severe hyperparathyroidism, in which early stop codons were present in both CaSR alleles, additional phenotypic disturbances included growth retardation, generalized osteopenia, and attenuated development of the cerebral white matter (5). The signaling pathways that underlie CaSR-mediated control of cell fate, however, are largely undefined.

We have previously reported that activation of CaSR results in the dual phosphorylation of AKT in osteoblasts (6). Phosphorylation of AKT at Thr^{308} is mediated by 3-phosphoinositide–dependent kinase 1 (PDK1) (7, 8) downstream of phosphatidylinositol 3-kinase (PI3K), whereas phosphorylation of AKT at Ser^{473} is mediated by the mechanistic target of rapamycin (mTOR) complex-2 (mTORC2), also known as PDK2 (9–11), a complex of proteins that specifically includes a rapamycin-insensitive companion of mTOR (Rictor), but not the regulatory-associated protein of mTOR (Raptor) (12). mTORC2-dependent Ser^{473} phosphorylation of AKT occurs independently of, and is required for, Thr^{308} phosphorylation (9). The upstream mechanism by which mTORC2 couples to the CaSR, however, is unknown. Recently it was shown that mTORC2 localizes to the plasma membrane, independently of PI3K, where it functions to phosphorylate AKT at Ser^{473} (13).

Canonical Wnt signaling in osteoblasts is a key determinant of bone cell fate and function (14, 15). The process depends on the binding of extracellular Wnt proteins, such as Wnt3a, to Frizzled-LDL receptor-related protein-5&6 (LRP5/6), inactivating glycogen synthase kinase-3 (GSK3) via plasma mem-

This work was supported by National Health and Medical Research Council of Australia Grant 1008282. The authors declare that they have no conflicts of interest with the contents of this article.

This article contains Figs. S1–S3 and Table S1.

[1] To whom correspondence may be addressed: Anderson Stuart Bldg., F13, Sydney University, Sydney, New South Wales 2006, Australia. Fax: 61-2-9351-2561; E-mail: rebecca.mason@sydney.edu.au.

[2] To whom correspondence may be addressed: Charles Perkins Centre (D17), University of Sydney, New South Wales 2006, Australia. E-mail: arthur.conigrave@sydney.edu.au.

[3] The abbreviations used are: CaSR, calcium-sensing receptor; AKT, acutely-transforming retrovirus AKT8 in rodent T-cell lymphoma; GPCR, G-protein–coupled receptor; mGluR, metabotropic glutamate receptor; CNS, central nervous system; PDK1, 3-phosphoinositide-dependent kinase 1; PI3K, phosphatidylinositol 3-kinase; mTOR, mechanistic target of rapamycin; mTORC1, mTOR complex 1; mTORC2, mTOR complex 2; Rictor, rapamycin-insensitive companion of mTOR; Raptor, regulatory associated protein of mTOR; LRP5/6, LDL receptor-related protein-5 and 6; ALP, alkaline phosphatase; ERK, extracellular signal-regulated kinase; OPG, osteoprotegerin; 4-pNPP, 4-nitrophenyl phosphate; FCS, fetal calf serum; DMEM, Dulbecco's modified Eagle's medium; DAPI, 4′,6-diamidino-2-phenylindole; IF, immunofluorescence; qPCR, quantitative PCR.

brane sequestration, resulting in the stabilization of cytoplasmic β-catenin that subsequently translocates to the nucleus where it promotes expression of genes under the control of TCF/LEF transcription factors (16). Independently of canonical Wnt-dependent inhibition of GSK3, AKT inhibits the kinase activity of GSK3 via direct phosphorylation at Ser^{21} (α-subunit) (17) and Ser^{9} (β-subunit) (18). Similarly, direct phosphorylation of β-catenin at Ser^{552} by AKT promotes its nuclear translocation and transcriptional activity (19).

We previously reported that activation of the CaSR in human osteoblasts resulted in the AKT-dependent translocation of β-catenin to the nucleus in primary human osteoblasts, thus potentially linking the AKT and Wnt/β-catenin pathways in bone cells (6). In agreement, Wnt3a-dependent activation of LRP5/6 in stromal ST2 cells activated the mTORC2/AKT pathway and promoted cell differentiation (20), showing that crosstalk between the pathways can potentially occur in both directions. However, the underlying mechanism by which the CaSR links to the mTORC2/AKT pathway in bone cells has not been defined.

Homer proteins act as scaffolds at the plasma membrane for the assembly of signaling complexes that include the family C metabotropic glutamate receptors mGluR1 and mGluR5 (21–23). The outcomes include cell fate determination via AKT (22, 24) and $ERK_{1/2}$ (23) and underlie neuroplasticity in the hippocampus and other areas of the CNS (25). Several Homer isoforms are recognized (26, 27). Among these, the long isoforms Homer1b and -1c (but not the short isoform 1a), as well as Homer2 and -3, contain coiled-coil domains that mediate self-multimerization and Ena/Vasp homology (EVH1) domains (present in all Homer isoforms) that mediate signaling interactions (28, 29). Disruption of Homer–mGluR1 interactions in mouse neurons decreased PI3K activity (24). Whether, in some cell contexts, Homer also supports CaSR-dependent activation of mTORC2 upstream of AKT is unknown.

In this study, we tested the hypothesis that in osteoblasts the long isoforms of Homer1 (hence referred to as Homer1) containing coiled-coil regions may link CaSR to mTORC2, resulting in activation of AKT and β-catenin stabilization in these cells (hypothesis shown schematically in Fig. 1).

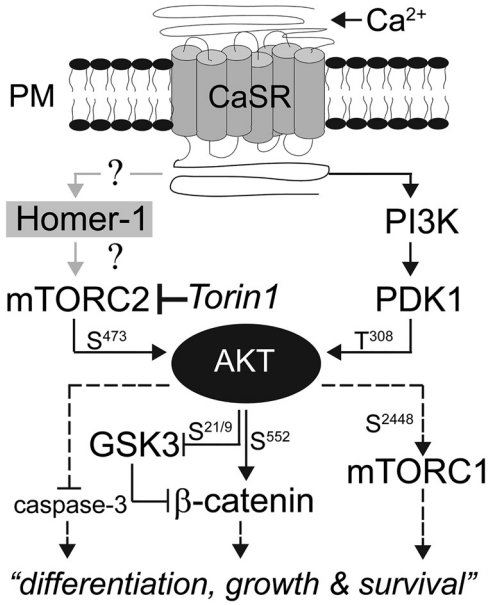

Figure 1. We propose Homer1 may link CaSR to mTORC2 in osteoblasts to promote AKT-dependent β-catenin stabilization. A proposal of this study is that Homer-1 may link CaSR to mTORC2 activation upstream of AKT (indicated by *?*). AKT phosphorylation is known to occur via two discrete mechanisms: PI3K-dependent phosphorylation at Thr^{308}, and mTORC2-dependent phosphorylation at Ser^{473}. AKT subsequently inhibits GSK3 and directly phosphorylates β-catenin to promote β-catenin stabilization and allowing subsequent nuclear translocation leading to cellular differentiation. AKT also suppresses apoptosis and promotes growth in the cell. Kinase target of Torin1 is mTOR. *PM* = plasma membrane.

Results

CaSR and Homer1-mediated extracellular Ca^{2+}-stimulated AKT signaling in osteoblasts

We first confirmed that activation of CaSR by its physiological ligand Ca^{2+} resulted in dual phosphorylation of AKT with phosphorylation of Ser^{473} preceding phosphorylation of Thr^{308} (Fig. 2*A*). Maximal phosphorylation at these sites was reached 15 min following exposure to elevated Ca^{2+} and was the time point used for all subsequent signaling analyses (Fig. 2*A*). Inhibition of mTORC2 with Torin1 decreased Ca^{2+}-stimulated phosphorylation of AKT at both Ser^{473} and Thr^{308} in a concentration-dependent manner (Fig. 2*B*). We confirmed that Torin1 treatment had no effect on mTORC1 at this early time point as evidenced by no change in mTORC1–Ser^{2448} phosphorylation, a marker of mTORC1 activity (Fig. 2*B*) (30). Therefore, changes in AKT phosphorylation in response to the inhibitor at this time point were not due to a previously reported phenomenon of negative feedback–dependent regulation of mTORC2 by mTORC1 (31, 32) but were due to inhibition of mTORC2 protein kinase activity *per se*.

We next hypothesized that Homer1 may mediate extracellular Ca^{2+}-induced mTORC2-dependent AKT signaling downstream of the CaSR in osteoblasts. Consistent with this hypothesis, when the expression of either the CaSR (Fig. 2, *C* and *D*) or Homer1 (Fig. 2, *E* and *F*) proteins was reduced selectively by specific siRNA in human osteoblasts, we observed decreased Ca^{2+}-dependent AKT phosphorylation at both Ser^{473} and Thr^{308} compared with control.

Homer1 and CaSR co-localized and co-immunoprecipitated in vitro with mTOR and the mTORC2-specific protein Rictor in response to elevated extracellular Ca^{2+}

Deconvolution microscopy of mouse bone sections revealed that CaSR and Homer1 were expressed in the same cells of mineralized bone (Fig. 3*A*, top row). As a comparison $CaSR^{-/-}$-mineralized bone sections are also shown (Fig. 3*A*, *bottom row*). Confocal microscopy of a monolayer culture of primary human osteoblasts stained for CaSR and Homer1 is shown in Fig. 3*B* (*top row*). A high-resolution image of a single osteoblast (Fig. 3*B*, *bottom row*) indicated co-localization (Pearson's coefficient = 0.41; below threshold = −0.02).

Because Homer1 was required for extracellular Ca^{2+}-dependent dual phosphorylation of AKT (Fig. 2, *E* and *F*), we hypothesized that Homer1 may interact with the CaSR and mTORC2 protein components, and we also tested whether any interaction might be dependent on an increase in extracellular Ca^{2+}

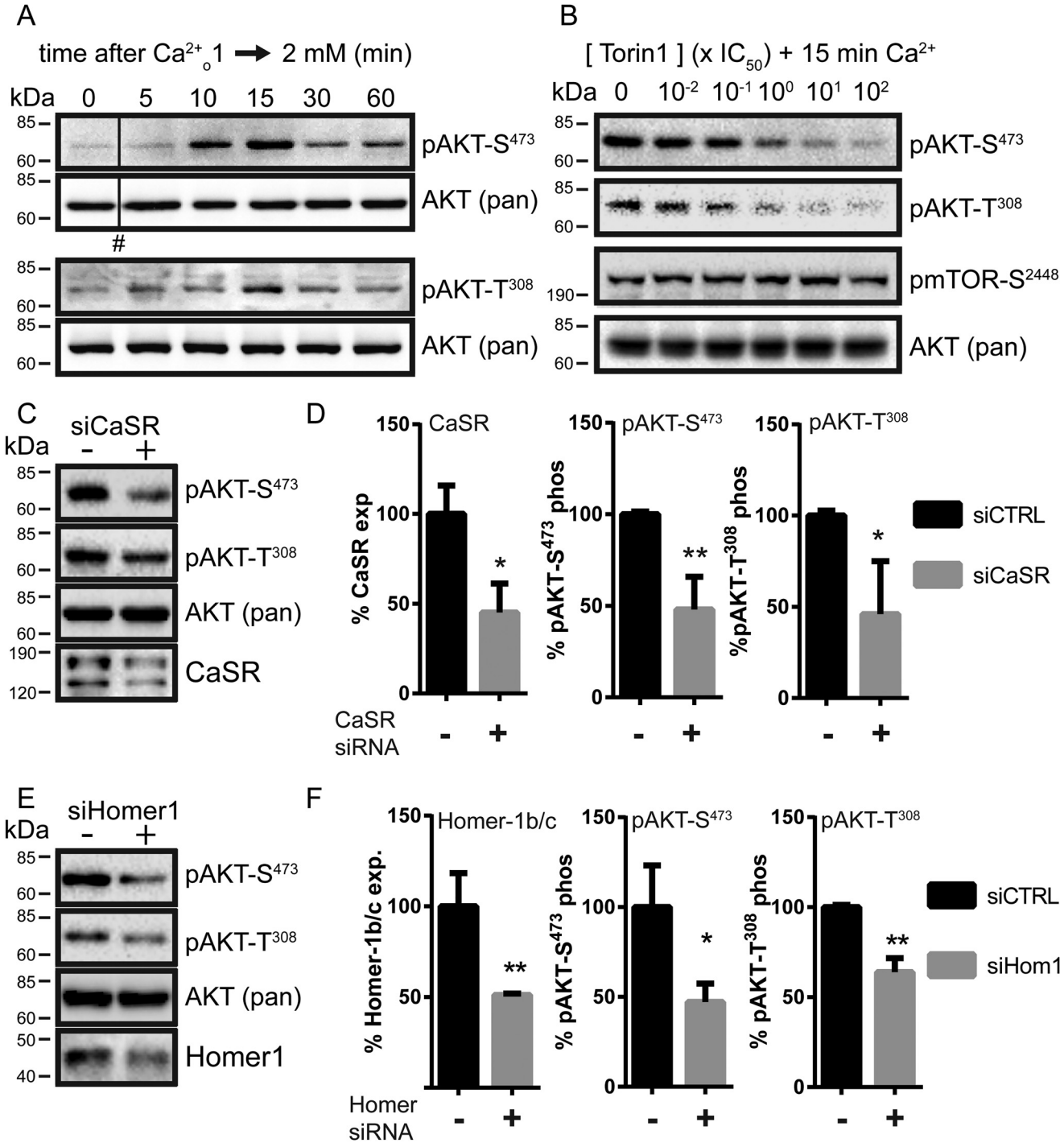

Figure 2. CaSR and Homer1 were necessary for mTORC2-dependent dual phosphorylation of AKT in response to elevated extracellular Ca^{2+} in osteoblasts. *A*, phosphorylations of AKT at Thr^{308}/Ser^{473} from same osteoblasts by Western blotting in response to $Ca^{2+}{}_o$ shift 1–2 mM over 1 h. *B*, Western blotting of AKT phosphorylated at Ser^{473}/Thr^{308} and mTOR phosphorylated at Ser^{2448} in response to $Ca^{2+}{}_o$ shift 1–2 mM for 15 min in the presence of Torin1 (pretreatment 5 min). Concentration is shown as fold times the half-maximal inhibitory concentration (IC_{50}). IC_{50} Torin1 ~2 nM. *C* and *E*, Western blotting of phosphorylations of AKT at Thr^{308}/Ser^{473}, in response to $Ca^{2+}{}_o$ shift 1–2 mM for 15 min after CaSR (siCaSR) (*C*) or Homer1 (siHomer1) (*E*) protein levels reduced (+) compared with control transfected cells (−). *D* and *F*, densitometry of triplicate blots shown for silenced CaSR (*C*) and Homer1 (*E*), respectively. #, *solid, vertical black lines* on the presented Western blotting indicate where lanes have been spliced from the same Western blotting for presentation purposes. The data shown in *C–F* are also presented in Fig. 4 as part of the broader signaling cascade investigated in the study. *, $p < 0.05$; **, $p < 0.01$.

concentration. After immunoprecipitation with an anti-Homer1 antibody, Homer1 was itself readily detected, and this was unaffected by an increase in extracellular Ca^{2+} concentration from 1.0 to 3.5 mM (Fig. 3, *C* and *D*, *ns*). Homer1 protein from nonimmunoprecipitated lysate is shown at the same molecular mass (~45 kDa, Fig. 3*C*). CaSR protein, at ~170 kDa, a molecular mass representing glycosylated, plasma membrane-associated CaSR (33) (Uniprot ID P41180), was detected in Homer1 immunoprecipitates, and the amount of CaSR bound to Homer1 *increased* in response to elevated Ca^{2+} (Fig.

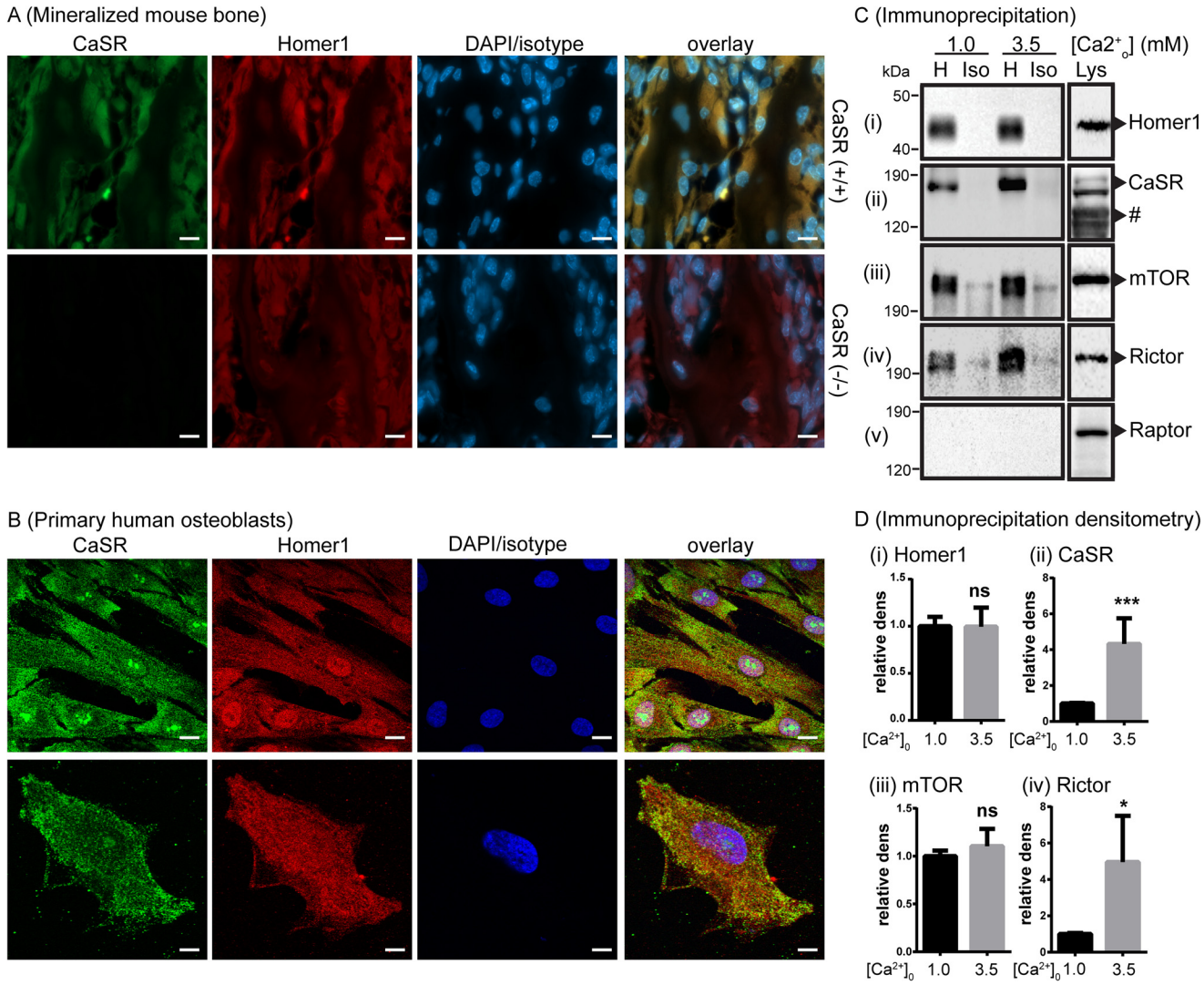

Figure 3. CaSR and Homer1 were co-expressed in mineralized bone, co-localized *in vitro*, and co-immunoprecipitated with mTOR and the mTORC2-specific protein Rictor. *A,* deconvolution microscopy images of the mineralized area of the long bones of WT (*top row*) or CaSR$^{-/-}$ (*bottom row*) mice stained for CaSR (*green*) or Homer1 (*red*). Nuclei (*blue*) stained with DAPI. ×63 objective. *Scale,* 50 μm. *B,* confocal microscopy images of a monolayer culture of primary human osteoblasts taken with ×10 objective (*top row, scale bar,* 10 μm) or a single osteoblast taken under oil with ×63 objective (*bottom row, scale bar,* 2 μm) stained for CaSR (*green*) or Homer (*red*). Nuclei (*blue*) were stained with DAPI. *C,* human osteoblasts were exposed to $Ca^{2+}{}_o$ shift 1–3.5 mM for 2 min and then lysed with a nonionic detergent. Soluble protein was immunoprecipitated with anti-Homer1 (*H*) or an isotype control (*Iso*). Detection of Homer1 (*panel i*), as a control between $Ca^{2+}{}_o$ treatments, CaSR (*panel ii*), mTOR (*panel iii*), Rictor (*panel iv*), and Raptor (*panel v*) by Western blotting from the immunoprecipitated fraction. Total lysate is Western blotting of nonimmunoprecipitated osteoblast lysate; # is nonglycosylated CaSR. *D,* densitometry from triplicate blots, where bands were detected, shown in *C* for Homer1 (*panel i*), CaSR (*panel ii*), mTOR (*panel iii*), and Rictor (*panel iv*). *ns,* no significance; *, $p < 0.05$; ***, $p < 0.001$.

3, *C* and *D*, $p < 0.001$). CaSR protein was present at 170 kDa in the osteoblast lysate (Fig. 3*C*, *CaSR*) and also at a lower molecular mass of ~120 kDa (Fig. 3*C*, *#*). This 120-kDa isoform corresponds to nonglycosylated endoplasmic reticulum/Golgi-associated CaSR, and was not immunoprecipitated with Homer1 (Fig. 3*C*).

mTOR and the mTORC2-specific protein Rictor were present in nonimmunoprecipitated osteoblast lysates (Fig. 3*C*) and were detected in Homer1 immunoprecipitates. In the case of mTOR, however, no Ca^{2+}-dependent increase in its level was observed (Fig. 3, *C* and *D, ns*), whereas Rictor protein levels, like those of the CaSR, increased in response to elevated extracellular Ca^{2+} (Fig. 3, *C* and *D*, $p < 0.05$). In contrast, although the mTORC1-specific protein Raptor was present in lysates (Fig. 3*C*), it was not detected in Homer1 immunoprecipitates at either control or elevated Ca^{2+} (Fig. 3*C*). Thus, in the presence of an elevated extracellular Ca^{2+} concentration, we observed increased association between the CaSR, Homer1, and the mTORC2-specific protein Rictor, but not the mTORC1-specific protein Raptor.

CaSR and Homer1 were required for extracellular Ca^{2+}-dependent β-catenin nuclear translocation following AKT activation in osteoblasts

We previously reported that the CaSR agonist strontium (Sr^{2+}) induced nuclear translocation of β-catenin in human osteoblasts following activation of AKT and demonstrated that these effects were mediated by the CaSR (6). Consistent with this observation, exposure of cells to elevated extracellular Ca^{2+} resulted in concentration-dependent phosphorylations of the inhibitory sites of GSK3α/β at Ser^{21}/Ser^{9}, respectively, and activator site of β-catenin at Ser^{552} (Fig. 4*A*), and nuclear trans-

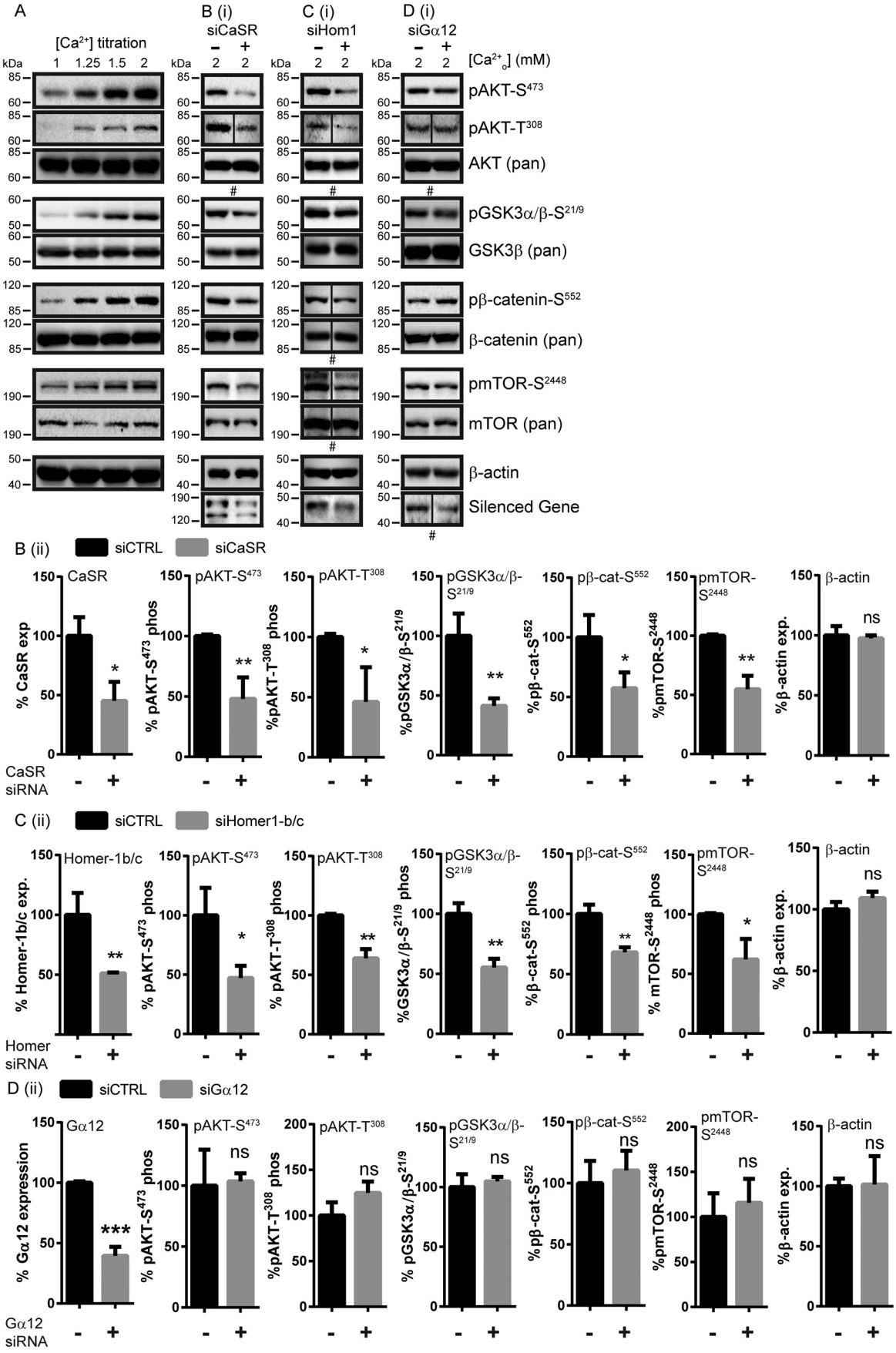
A
[Ca2+] titration
1 1.25 1.5 2
B (i)
siCaSR
C (i)
siHom1
D (i)
siGα12
[Ca2+o] (mM)
pAKT-S473
pAKT-T308
AKT (pan)
pGSK3α/β-S21/9
GSK3β (pan)
pβ-catenin-S552
β-catenin (pan)
pmTOR-S2448
mTOR (pan)
β-actin
Silenced Gene
B (ii)
siCTRL
siCaSR
CaSR
% CaSR exp
% pAKT-S473 phos
%pAKT-T308 phos
%pGSK3α/β-S21/9
%pβ-cat-S552
%pmTOR-S2448
%β-actin exp.
ns
CaSR siRNA
C (ii)
siHomer1-b/c
Homer-1b/c
% Homer-1b/c exp.
% pAKT-S473 phos
% pAKT-T308 phos
%GSK3α/β-S21/9 phos
%β-cat-S552 phos
% mTOR-S2448 phos
Homer siRNA
D (ii)
siGα12
Gα12
% Gα12 expression
Gα12 siRNA

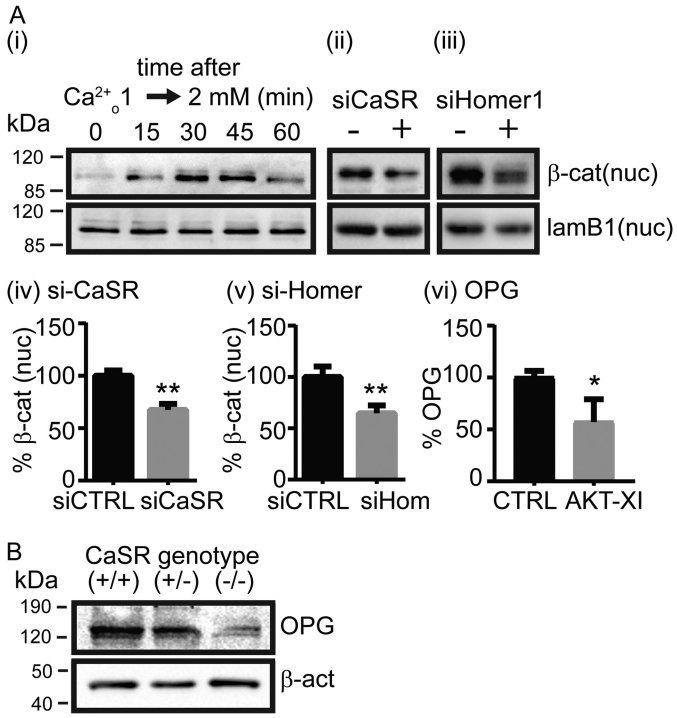

Figure 5. CaSR and Homer1-modulated Ca^{2+}-dependent β-catenin nuclear translocation in human osteoblasts. *A,* nuclear β-catenin (*β-cat*) is shown in response to *panel i*, $Ca^{2+}{}_o$ shift from 1 to 2 mM over a 60-min period, or *panels ii* and *iii,* a 30-min $Ca^{2+}{}_o$ shift 1 to 2 mM with reduction in CaSR protein level (*siCaSR*; *panel ii*) or reduction in Homer1 protein level (*siHomer1*; *panel iii*) by siRNA. The nuclear (*nuc*) protein laminB1 (*lamB1*) was used as a loading control for the nuclear fraction. *Panels iv* and *v,* densitometry from triplicate blots for silenced CaSR and Homer1. *Panel vi,* OPG protein levels, corrected for total cell protein, measured by whole-cell ELISA in cells that were incubated for 24 h in 2 mM $Ca^{2+}{}_o$ ± AKT kinase inhibitor AKT-XI (20 μM). *B,* Western blotting of OPG that was chemically extracted from marrow flushed mouse long bones from WT (*CaSR*+/+), heterozygous (*CaSR*+/−), or CaSR knockout (*CaSR*−/−). β-Actin loading control. *, $p < 0.05$; **, $p < 0.01$.

location of β-catenin, as demonstrated by Western blotting of nuclear fractions at various times over 60 min (Fig. 5*A*, *panel i*). The phosphorylation of mTOR at Ser^{2448} (carried out by p70S6K and indicative of mTORC1 activation downstream of AKT (30)) was also stimulated by elevated extracellular Ca^{2+} (Fig. 4*A*).

Osteoblasts transfected with siRNA directed against the CaSR exhibited decreased CaSR protein expression (Fig. 4*B*, *panel i, bottom row,* and *panel ii*, $p < 0.05$), and knockdown of the CaSR attenuated the stimulatory effect of elevating extracellular Ca^{2+} on the phosphorylations of AKT–Ser^{473} ($p < 0.01$), AKT–Thr^{308} ($p < 0.05$), GSK3α/β–Ser^{21}/Ser^{9} ($p < 0.01$), β-catenin–Ser^{552} ($p < 0.05$), and mTOR–Ser^{2448} ($p < 0.01$) (Fig. 4*B*, *panel i* for Western and *panel ii* for significance) as well as nuclear localization of β-catenin (Fig. 5*A*, *panels ii* and *iv*, $p < 0.01$).

Table 1

Quantitative RT-PCR microarray analysis of the impact of CaSR depletion on the expression of various genes of the canonical Wnt pathway

Total RNA was extracted from marrow-flushed 2.3Col(I)-CaSR and WT bone and analyzed with the Wnt Signaling Pathway array kit (SuperArray Bioscience). *p* value was generated by *t* test.

Gene	ΔΔ*Ct*	Expression fold change ($2^{\wedge}$-ΔΔ*Ct*) $CaSR^{-/-}$/WT	*p* value
Axin1	0.56	0.68	0.032
Ccnd3	1.02	0.49	0.017
Csnk2a1	0.71	0.61	0.011
Ctnnb1	0.36	0.78	0.019
Daam1	0.96	0.52	0.011
Dvl2	0.43	0.74	0.042
Jun	0.64	0.64	0.001
Kremen1	0.22	0.86	0.028
Lef1	0.89	0.54	0.011
Lrp5	1.04	0.49	0.012
Nkd1	1.20	0.44	0.004
Tcf7	0.49	0.71	0.043
Wif1	0.97	0.51	0.033
Wisp1	1.00	0.50	0.005
Wnt1	2.10	0.23	0.002
Wnt10a	1.20	0.44	0.004
Actb(control)	0.02	0.99	0.52
Gusb(control)	−0.6	1.52	0.076

Osteoblasts transfected with siRNA directed against Homer1 exhibited decreased Homer1 protein expression (Fig. 4*C*, *panel i, bottom row,* and *panel ii*, $p < 0.01$), and knockdown of Homer1 also attenuated the stimulatory effect of elevated extracellular Ca^{2+} on the phosphorylations of AKT–Ser^{473} ($p < 0.05$), AKT–Thr^{308} ($p < 0.01$), GSK3α/β–Ser^{21}/Ser^{9} ($p < 0.01$), β-catenin–Ser^{552} ($p < 0.01$), and mTOR–Ser^{2448} ($p < 0.05$) (Fig. 4*C*, *panel i* for Western and *panel ii* for significance) as well as nuclear translocation of β-catenin (Fig. 5*A*, *panel iii* and *panel v*, $p < 0.01$).

Taken together, these observations indicate that the CaSR and Homer1 were required for extracellular Ca^{2+} stimulation of an AKT-dependent pathway that controlled β-catenin translocation. To separately confirm the role of AKT on the nuclear translocation of β-catenin *in vitro*, chemical inhibition of AKT with AKT-XI (20 μM) reduced osteoprotegerin (OPG) expression, a marker of the LEF/TCF pathway (Fig. 5*A*, *panel vi*) (15). A degree of CaSR control of β-catenin stabilization and translocation was also apparent *in vivo* as $CaSR^{-/-}$ mice had reduced protein levels of the Wnt marker OPG compared with WT (Fig. 5*B*). Similarly, qPCR analysis also showed that the mRNA levels of several Wnt-responsive genes in $CaSR^{-/-}$ mice were reduced compared with WT (Table 1).

As a control for the signaling analysis and to assess potential off-target effects, siRNA was used to knock down $G\alpha_{12}$, a protein that does not affect AKT but inhibits $ERK_{1/2}$ in osteoblasts (34, 35). Silencing $G\alpha_{12}$ resulted in reduced $G\alpha_{12}$ protein (Fig. 4*D*, panel i, bottom row, and *panel ii*, $p < 0.001$) and, as expected, further increased Ca^{2+}-induced $ERK_{1/2}$ phosphory-

Figure 4. CaSR and Homer1 modulated Ca^{2+}-dependent activation of the AKT pathway in human osteoblasts. *A–D,* phosphorylation of AKT at Ser^{473}/Thr^{308}, GSK3α–Ser^{21}, GSK3β–Ser^{9}, β-catenin–Ser^{552}, mTOR–Ser^{2448}, and β-actin (loading control) from human osteoblasts by Western blotting. *A,* osteoblasts exposed to various $Ca^{2+}{}_o$ concentrations for 15 min. *B–D, panel i,* osteoblasts were exposed to $Ca^{2+}{}_o$ shift from 1–2 mM for 15 min after silencing: *B,* CaSR (*siCaSR*); *C,* Homer1 (*siHom1*); *D,* Gα12 (*siGα12*) (+), and the lysates were then processed for Western blotting detection of various proteins and phosphoproteins as shown. The impact of siRNA on the silenced gene is shown at the *bottom of each column* in each of *B* (*panel i*), *C* (*panel i*), and *D* (*panel i*), where expression is shown as "silenced gene." For each transfection, the effect of a nondirected control siRNA sequence (*siCTRL*) is shown (−). *B* and *C, panel ii,* densitometry results from triplicate blots shown *B* (*panel i*), *C* (*panel i*), and *D* (*panel i*). *, $p < 0.05$; **, $p < 0.01$, *ns,* not significantly different. # *Solid, vertical black lines* on the presented Western blotting indicate where lanes have been spliced from the same Western blotting for presentation purposes. The AKT, CaSR, and Homer1 data shown in *B* and *C* are also shown in Fig. 2, which focuses independently on AKT.

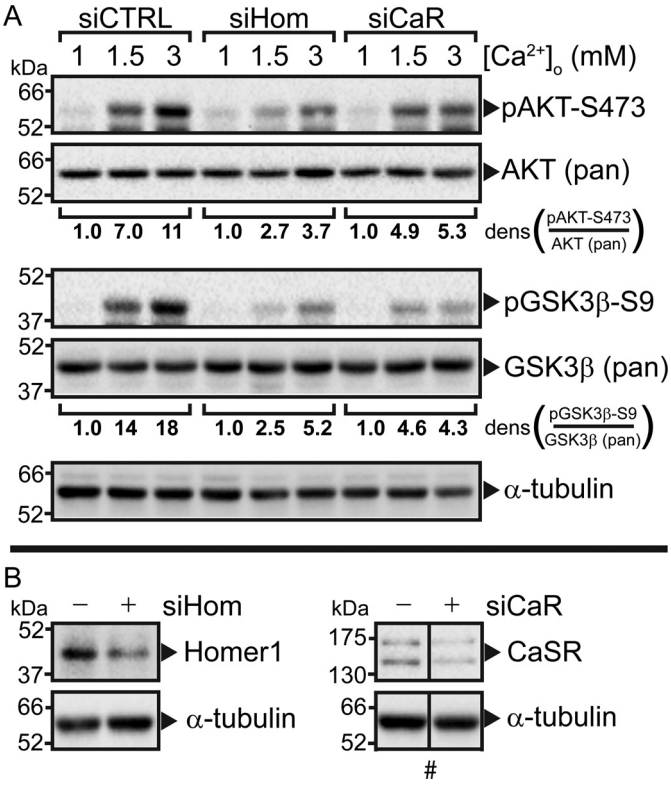

Figure 6. CaSR and Homer1-modulated Ca^{2+}-dependent phosphorylation of AKT–Ser^{473} and GSK3β–Ser^{9} in MG63 osteosarcoma cells. *A,* Western blotting showing level of AKT–Ser^{473}/total AKT (pan), GSK3β–Ser^{9}/total GSK3β (pan), and α-tubulin (loading control) in response to various $Ca^{2+}{}_o$ concentrations for 15 min in MG63 osteosarcoma cells. Prior to $Ca^{2+}{}_o$ treatment, cells were transfected with siRNA directed at Homer1 (*siHom*), CaSR (*siCaR*), or a nondirected sequence (*siCTRL*) for 48 h. Densitometry values (*dens*) were calculated by dividing the detected level of phosphorylated protein by the level of total protein (ImageJ), and normalizing this number to the ratio obtained from the 1 mM $Ca^{2+}{}_o$ *lane* for each silenced condition. *B,* Western blotting showing expression level of Homer1 and CaSR in response to each directed siRNA (+) compared with cells transfected with a nondirected sequence (−) in MG63 cells. # *Solid, vertical black lines* on the presented Western blotting (*B, panel,* siCaR blots only) indicate where lanes have been spliced from the same Western blotting for presentation purposes. The experiment was independently repeated with similar results.

lation (Fig. S1). However, knockdown of $G\alpha_{12}$ had no effect on the phosphorylations of AKT at Ser^{473} or Thr^{308} or of its key downstream targets, including GSK3, β-catenin, or mTORC1 as revealed by p70 S6K-dependent phosphorylation of mTOR at Ser^{2448} (Fig. 4*D*, panel i for Western, and *panel ii* for significance).

CaSR and Homer1 were required for extracellular Ca^{2+}-dependent AKT and GSK3β phosphorylation in MG63 osteosarcoma cells

The effect of Homer1 and CaSR on the phosphorylation of AKT–Ser^{473} and GSK3β–Ser^{9} in response to elevated extracellular Ca^{2+} was also examined in a second osteoblast cell type, the commonly used osteosarcoma cell line MG63. We found that Homer1 and CaSR were expressed in MG-63 cells (Fig. 6). In these cells, both AKT–Ser^{473} and GSK3β–Ser^{9} phosphorylation were increased in response to elevated extracellular Ca^{2+}, and siRNA-dependent knockdown of either Homer1 or CaSR clearly reduced the phosphorylation level of both proteins in response to $Ca^{2+}{}_o$ (Fig. 6). These findings were consistent with our analyses performed in primary human osteoblasts (Fig. 4).

Effect of CaSR and Homer1 on cell fate of osteoblasts

Given the observed effect of the CaSR and Homer1 on Ca^{2+}-stimulated nuclear β-catenin translocation (Fig. 5), which promotes differentiation in osteoblasts (15), we next investigated whether the CaSR and Homer1 modulated alkaline phosphatase (ALP) activity, another marker of osteoblast differentiation (36). Elevated extracellular Ca^{2+} (1.0–2.0 mM) stimulated ALP activity by 4–5-fold after 3 days (Fig. 7*A*, $p < 0.01$). Silencing the CaSR abolished the stimulatory effect of elevated Ca^{2+} (2.0 mM) on ALP activity but had no effect on basal ALP activity (Fig. 7*B*). Silencing Homer1 suppressed basal ALP activity in cells exposed to control extracellular Ca^{2+} (1.0 mM, $p < 0.05$) and abolished the response to elevated Ca^{2+} (2.0 mM) (Fig. 7*C*), demonstrating that Homer1 supports a key function of differentiated osteoblasts in the physiologically relevant extracellular Ca^{2+} concentration range.

Finally, we investigated the roles of CaSR and Homer1 in AKT-dependent osteoblast survival in the presence of pro-apoptotic oxidative stress, an important determinant of viability *in vivo* (37), using caspase-3 activity as the readout. Elevated extracellular Ca^{2+} suppressed oxidative stress-induced elevations of caspase-3 activity in a concentration-dependent manner from 1 to 2 mM (Fig. 7*D*), and the prosurvival effect of elevated Ca^{2+} was reversed upon silencing either the CaSR (Fig. 7*E*) or Homer1 (Fig. 7*F*). Furthermore, downstream of CaSR and Homer1, mTORC2-dependent phosphorylation of AKT–Ser^{473} (9) was clearly critical in this action of extracellular Ca^{2+}, because the inhibitor Torin1 caused significant concentration-dependent increases in caspase-3 activity in the presence of 2 mM Ca^{2+} and the oxidative stressor 125 μM H_2O_2 (Fig. 7*G*), whereas wortmannin, the inhibitor of PI3K upstream of AKT, had no effect (Fig. 7*H*).

Transfection of Homer-1c into HEK-293 cells stably expressing CaSR established AKT–Ser^{473} sensitivity to extracellular Ca^{2+}

It is possible that the CaSR–Homer1–mTORC2 complex identified in osteoblasts in this study operates more widely in other cell types that express both the CaSR and Homer1. To test this hypothesis, we performed experiments in the human embryonic kidney cell line, HEK-293, and HEK-293 cells stably expressing CaSR (HEK-CaSR), a well-established cellular system for studies of CaSR signaling (38, 39).

Transient transfection of control HEK-293 cells with *Homer1c* (HEK-Homer1c) resulted in maximal Homer1c protein expression 48 h post-transfection (Fig. 8*A*). Exposure of control HEK-CaSR cells to various $Ca^{2+}{}_o$ concentrations in the range of 0.1–5 mM for 15 min yielded no increase in AKT–Ser^{473} phosphorylation (Fig. 8*B*). Similarly, HEK-293 cells transiently transfected with only Homer1c (in the absence of CaSR) failed to respond to raised extracellular Ca^{2+} with AKT–Ser^{473} phosphorylation (Fig. 8*C*). However, when HEK-CaSR cells were transiently transfected with *Homer1c*, $Ca^{2+}{}_o$-dependent AKT–Ser^{473} sensitivity was observed (Fig. 8*D*). Therefore, both Homer1c and CaSR were required for $Ca^{2+}{}_o$-stimulated AKT–Ser^{473} phosphorylation in HEK-293 cells.

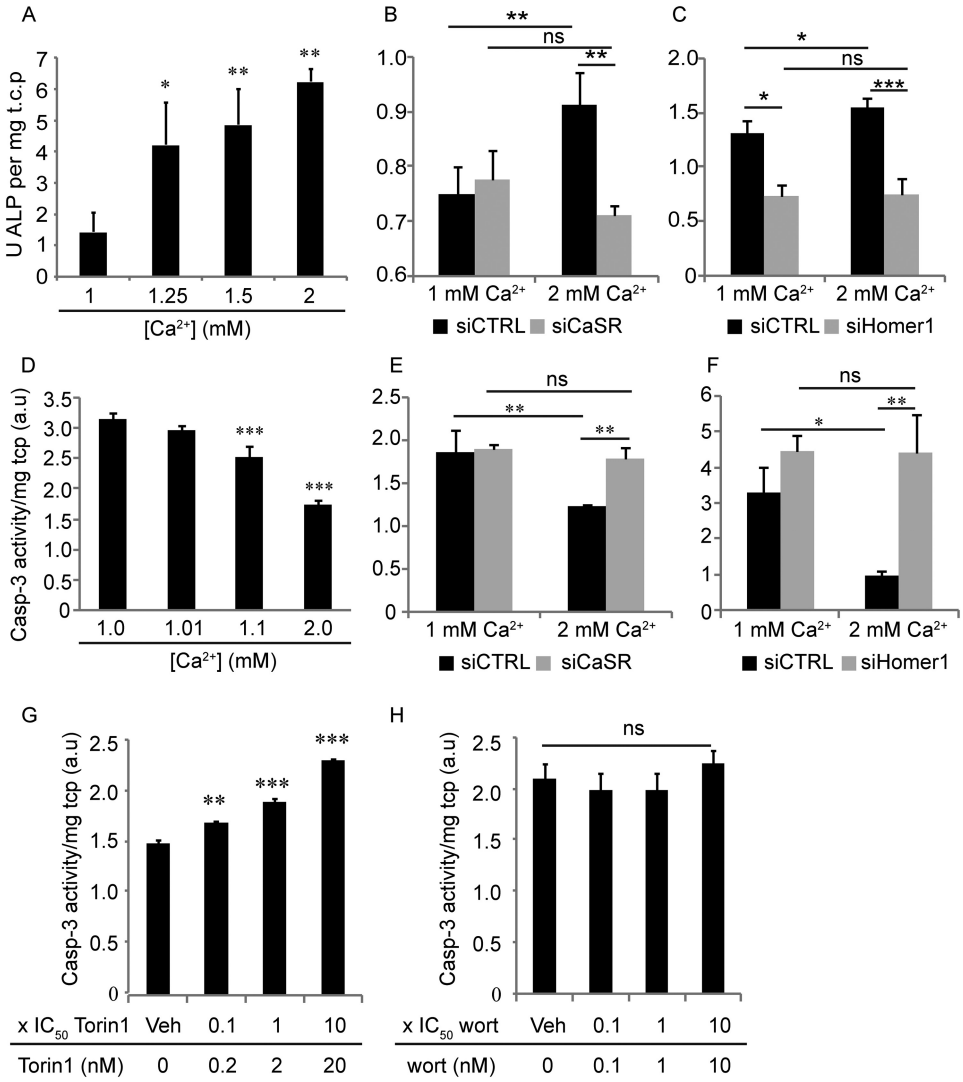

Figure 7. Ca^{2+}-dependent stimulation of alkaline phosphatase activity and rescue from oxidative stress–induced apoptosis depend on Homer1 and CaSR. ALP activity in response to various Ca^{2+} concentrations for 3 days in absence of siRNA (*A*), presence of siRNA to CaSR (*siCaSR)* (*B*), and presence of siRNA to Homer1 (*siHomer1*) (*C*). For each transfection, the effect of a nondirected control siRNA sequence (*siCTRL*) is shown. ALP corrected for total cellular protein *(t.c.p*). *D* and *E,* caspase-3 activity in osteoblasts treated with Ca^{2+} (*D*) at indicated concentrations for 5 h then 125 μM H_2O_2 for 2.5 h. *E* and *F,* osteoblasts transfected with siRNA to reduce CaSR (*siCaSR*) (*E*) or Homer1 (*siHomer1*) (*F*) or a nondirected control sequence (*siCTRL*) and then treated with 2 mM Ca^{2+} or vehicle (1 mM Ca^{2+}) for 5 h then 125 μM H_2O_2 for 2.5 h. *G* and *H,* caspase-3 in osteoblasts treated with 2 mM Ca^{2+} and Torin1 (IC_{50} ~2 nM) (*G*) or wortmannin (IC_{50}~1 nM) (*H*) for 5 h and then 125 μM H_2O_2 for 2.5 h. Caspase-3 corrected for t.c.p. *ns,* not significant, *, $p < 0.05$; **, $p < 0.01$; ***, $p < 0.001$ compared with vehicle (*Veh*).

Summary of results

We made several novel observations in this study. Homer1 protein was expressed in human osteoblasts. In mineralized mouse bone sections of WT mice, high levels of CaSR expression were associated with high levels of Homer1 expression. In agreement with this observation, confocal microscopy in primary human osteoblasts demonstrated co-localization of Homer1 and CaSR. Homer1 and the mature, glycosylated isoform of CaSR were shown to exist in a protein complex with mTOR and the mTORC2-specific protein Rictor by immunoprecipitation, and the level of CaSR and Rictor protein in the complex with Homer1 was significantly increased in response to increased extracellular calcium. Homer1 and CaSR modulated Ca^{2+}-induced AKT phosphorylation and the attendant translocation of β-catenin to the nucleus within 15 min of treatment. In MG63 osteosarcoma cells, which expressed both CaSR and Homer1, phosphorylation of AKT–Ser^{473} and GSK3β–Ser^{9} were increased in response to extracellular Ca^{2+}, whereas siRNA directed at either Homer1 or CaSR attenuated these effects. As predicted from the above signaling studies, both Homer1 and CaSR positively modulated osteoblast differentiation and resistance to stress-induced apoptosis. Taken together, these studies have established a novel CaSR–Homer1–mTORC2–AKT-signaling pathway in osteoblasts with functional consequences for cellular maturation and survival. In addition, we were able to establish reconstituted AKT–Ser^{473} sensitivity to extracellular Ca^{2+} in a nonosteoblast cell line. Thus, independent transfections of either Homer1 or CaSR into HEK-293 cells showed no AKT–Ser^{473} sensitivity to extracellular Ca^{2+}, however co-transfection of Homer1 and CaSR established AKT–Ser^{473} sensitivity to extracellular Ca^{2+}.

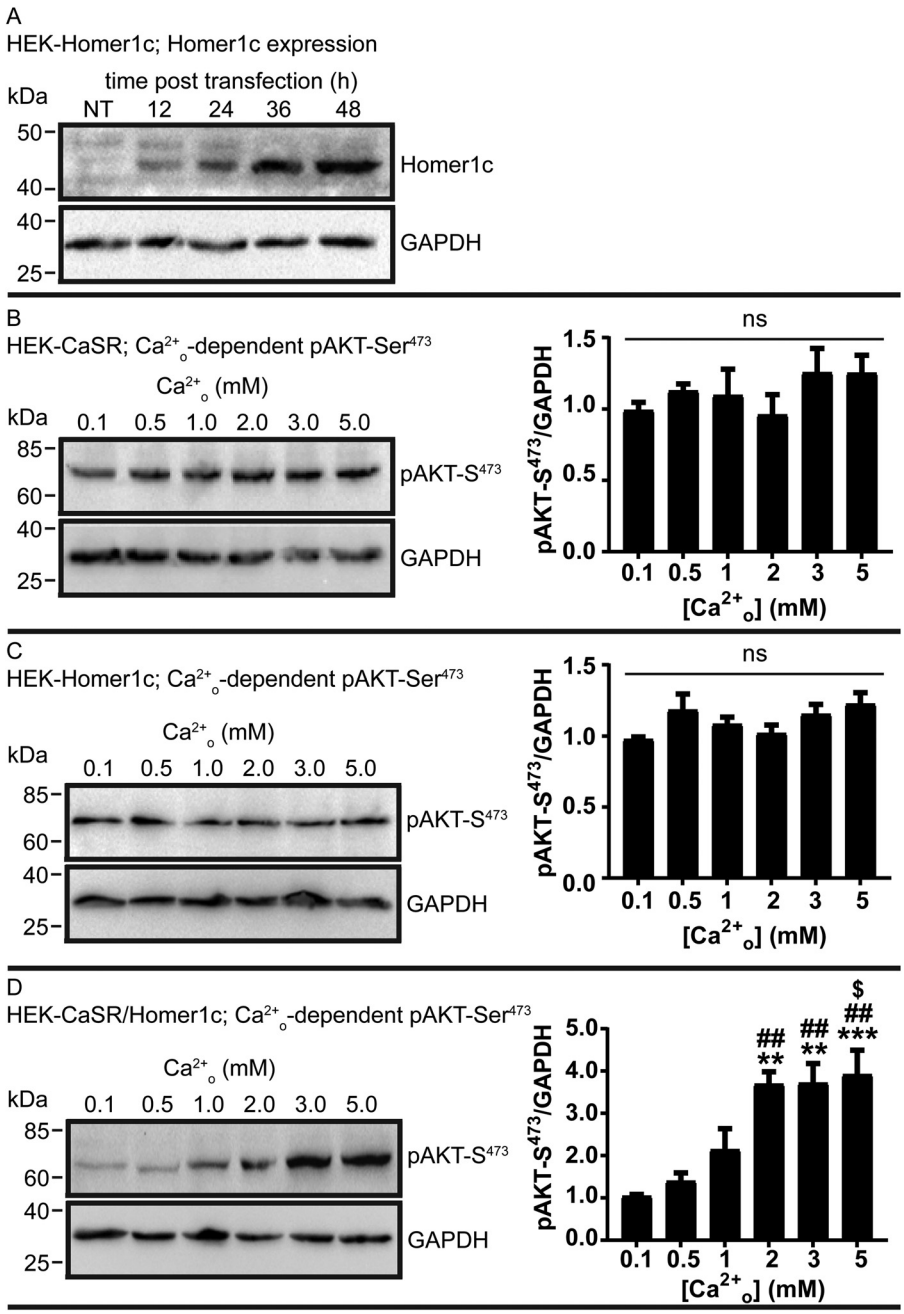

Figure 8. Co-transfection of HEK-293 cells with CaSR and Homer1c established AKT–Ser^{473} sensitivity to extracellular Ca^{2+}. *A,* Western blotting of HEK-293 cells transiently transfected with *Homer1c* (*HEK-Homer1c*) or nontransfected cells (*NT*) as a control, showing Homer1c protein levels at various time points post-transfection. 48 h post-transfection was chosen as the time point for subsequent signaling analyses *B–D,* Western blotting of AKT–Ser^{473} phosphorylation levels in response to 0.1–5 mM extracellular Ca^{2+} in HEK-CaSR (*B*), HEK-293 cells (*C*) transiently transfected with *Homer1c*, or HEK-CaSR cells (*D*) transiently transfected with *Homer1c*. *ns*, not significantly different; **, $p < 0.01$; ***, $p < 0.001$ compared with 0.1 mM $Ca^{2+}{}_o$; ##, $p < 0.01$ compared with 0.5 mM $Ca^{2+}{}_o$; $, $p < 0.05$ compared with 1 mM $Ca^{2+}{}_o$.

Discussion

Phosphorylation of AKT at Ser^{473} is mediated by mTORC2 (9), and our earlier studies showed that activation of the CaSR induces AKT Ser^{473} phosphorylation and nuclear β-catenin translocation in osteoblasts (6). This study extends these findings to show that Homer1 acts as a previously unrecognized link between the CaSR and mTORC2 upstream of AKT–Ser^{473} (Fig. 1). The proposal that Homer proteins, which primarily reside at the plasma membrane (21–23), promote AKT phosphorylation is consistent with the recent finding that mTORC2 assembles at the plasma membrane prior to phosphorylating AKT at Ser^{473} (13).

In this study, we observed that in the mineralized bone of WT mice areas exhibiting high levels of CaSR expression also exhibited high levels of Homer1 expression, and confocal microscopy of primary human osteoblasts demonstrated co-localization at the cellular level. Homer1 mediates PIKE-L–dependent activation of PI3K upstream of AKT–Thr^{308} phosphorylation in hippocampal neurons (22), but a mechanism dependent on Homer1 and mTORC2 has not been described

previously for the activation of AKT–Ser^{473}. We observed that CaSR-mediated AKT–Ser^{473} phosphorylation, the resultant downstream phosphorylations of GSK3β and β-catenin, and the attendant nuclear translocation of β-catenin are all dependent on Homer1. These observations provide a molecular explanation for CaSR-stimulated stabilization of β-catenin in osteoblasts (Fig. 1) (6). The requirement for CaSR and Homer1 to observe increased phosphorylation of both AKT–Ser^{473} and GSK3β–Ser^{9} in response to extracellular Ca^{2+} was also shown to be present in another commonly used osteoblast cell type, MG63 osteosarcoma cells.

It is not yet clear whether the interaction between the CaSR and Homer1 arises from a direct binding interaction or indirectly via an intermediate protein. In addition to the class C GPCRs mGluR1 and mGluR5 (21–23, 29), Homer1 interacts with the scaffolding protein SHANK1 as well as components of the actin cytoskeleton and cell signaling apparatus (27). For some of these interacting proteins, the Homer1-binding sequences have not yet been identified. A widely recognized consensus binding sequence PP*XX*F (25, 40), which is present in the C termini of both mGluR1 and mGluR5, is not present in the CaSR. However, some related sequences are present in the CaSR, including PTSF in intra-loop2 (residues 711–714; Uniprot P41180), and PENF in intra-loop3 (residues 799–802), which conform to a proposed variant of the consensus Homer1-binding sequence P*XX*F (22). Interestingly, the latter sequence is conserved in other members of GPCR family C, including mGluR1 and mGluR5 (Uniprot Q13255 and P41594, respectively). Two other proteins that interacted with the Homer1–CaSR complex in this study, mTOR and Rictor (Fig. 2), also contain Homer-binding sequences. mTOR contains the classical Homer1-binding sequence, PPKDF (residues 464–468, Uniprot P42345), and Rictor contains the variant sequence, PKGF (residues 812–815, Uniprot Q6R327).

We previously found that AKT stimulation in osteoblasts, downstream of the activated CaSR, promoted β-catenin stabilization and subsequent nuclear translocation that was dependent, in part, on inhibition of GSK3β activity via Ser^{9} phosphorylation and that chemical inhibition of AKT by AKT-XI halted this process (6). We confirmed these findings in this study and observed that the inhibitory phosphorylation sites of GSK3 were also suppressed by the mTOR kinase inhibitor Torin1 but not the PI3K inhibitor wortmannin (Fig. S2), highlighting the relative importance of mTORC2- *versus* PI3K-dependent control of AKT.

Increases in the osteoblast differentiation marker ALP in response to extracellular Ca^{2+} were suppressed by silencing both CaSR and Homer1 in this study. It is of note that basal levels of ALP were suppressed by Homer1 silencing but not CaSR silencing. One interpretation of this finding is that Homer1 performs functions essential to cell differentiation, other than those that respond to increases in extracellular Ca^{2+}. Clearly, CaSR is essential to normal osteoblast differentiation (1, 2); however, the role of Homer1 is not known in bone cells. To further investigate, we performed a direct comparison between silencing CaSR and Homer1 on osteoblast viability in response to hydrogen peroxide–induced stress as measured by the viability dye Cell Titer Blue (Fig. S3). Silencing Homer1 reduced osteoblast viability, and the effect exceeded that observed in cells in which the CaSR had been silenced. The results of this experiment are consistent with the hypothesis that Homer1 is a key mediator of prosurvival pathways in bone cells and warrants further investigation.

Resistance to oxidative stress promotes bone quality *in vivo* (41). Reducing the level of either CaSR or Homer1 with siRNA significantly reduced the ability of elevated extracellular Ca^{2+} to support cell survival in the context of oxidative stress or sparse culture conditions. Hydrogen peroxide–induced apoptosis increased in response to Torin1, which inhibited mTORC2 and thus AKT–Ser^{473} phosphorylation but was unaffected by wortmannin that inhibits PI3K, supporting the idea that mTORC2-induced phosphorylation of AKT, downstream of CaSR and Homer1, is a determinant of osteoblast survival.

The key observations of this study indicate the existence of a receptor-scaffolding protein–intracellular protein kinase mechanism in support of cell survival and differentiation in Ca^{2+}-stimulated osteoblasts that requires the CaSR, Homer1, mTORC2, and AKT. To further explore whether these interactions might be generalizable to other cell types, we investigated whether it might be possible to reconstitute extracellular Ca^{2+}-stimulated AKT–Ser^{473} phosphorylation in HEK-293 cells. Consistent with our primary cell findings, Ca^{2+}-stimulated AKT–Ser^{473} phosphorylation was not observed in HEK-293 cells that had been stably transfected with the CaSR or in HEK-293 cells that had been transiently transfected with Homer1c alone. However, in HEK–CaSR cells that were transiently transfected with Homer1c for the optimal period of 48 h, we observed reconstitution of extracellular Ca^{2+}-stimulated AKT–Ser^{473} phosphorylation that exhibited an EC_{50} for Ca^{2+} of 1.0–2.0 mM and a maximal response at $Ca^{2+}{}_o$ concentrations around 3–5 mM. HEK-293 cells have been reported previously to endogenously express both Rictor (42) and mTOR (42, 43), and we used Western blot analysis to confirm this in this study (data not shown). These observations, together with the observed impact of Homer1 knockdown in osteoblasts and osteosarcoma cells, indicate that expression of Homer1 in CaSR-expressing cells is required for the establishment of Ca^{2+}-stimulated AKT–Ser^{473} phosphorylation.

In conclusion, this study demonstrates that in response to extracellular Ca^{2+}, a novel protein complex, composed of CaSR, Homer1, and mTORC2, forms in human osteoblasts and mediates a pathway that controls the phosphorylation of AKT leading to increased differentiation and survival (Fig. 1). AKT phosphorylation supports an alternative pathway to the stabilization and nuclear translocation of β-catenin, a key driver of bone anabolism (15). This pathway may provide alternative targets for the development of new osteoporosis therapies. The findings demonstrate that in addition to roles in supporting neuromodulation and neuroplasticity by type-1 metabotropic glutamate receptors, Homer1 supports the control of bone cell survival and differentiation downstream of the CaSR, which monitors the levels of Ca^{2+} in the bone microenvironment.

Experimental procedures

Materials

All chemicals, including culture media, were obtained from Sigma unless otherwise specified. Fetal calf serum (FCS) and OptiMEM™ were from Life Technologies, Inc. All siRNA was from Santa Cruz Biotechnology. Protein A/G PLUS–agarose beads were from Santa Cruz Biotechnology. VeriBlot secondary antibodies were from Abcam. The inhibitor Torin1 was from Tocris (Bristol, UK), and wortmannin was from Sigma. The bicinchoninic acid (BCA) assay was obtained from Pierce. Caspase-3 fluorogenic substrate, *N*-acetyl-L-α-aspartyl-L-α-glutamyl-L-valyl-*N*-[2-oxo-4-(trifluoromethyl)-2*H*-1-benzopyran-7-yl]-L-α-asparagine (Ac-DEVD-AFC), was from Pharmingen. ALP substrate 4-nitrophenyl phosphate (4-pNPP) was from Sigma. ALP (calf, intestinal) was from Promega. All absorbance and fluorescence measurements were carried out on a CLARIOstar microplate reader (BMG Labtech GmbH, Germany). Sonication of cell lysates was performed using a Branson Analog 250 cell disruptor with a double step (1/8 inch) microtip from Branson Ultrasonics.

Methods

Cell culture—Human osteoblasts were grown from the minced trabecular ends of the fetal long bone in accordance with the National Health and Medical Research Council guidelines and with the approval of the University of Sydney Human Ethics Committee (approval number 2012/043), as described previously (6, 44–46). Each experiment was conducted using human osteoblasts from at least two different donors, and cells were maintained routinely in DMEM containing 10% (v/v) FCS. These bone-derived cells were moderately differentiated as described previously (6, 44). Because the bone cells were from different donors, some biological variations in responses were observed, as expected (6, 44, 45). HEK-293 (ATCC® CRL-1573) and MG-63 osteosarcoma cells (ATCC® CRL-1427) were maintained in DMEM containing 10% (v/v) FCS. The stably-expressed WT human CaSR in HEK-293 cells was the kind gift of Dr. Karen Krapcho and Dr. Edward Nemeth (NPS Pharmaceuticals).

CaSR knockout mice—Male and female mice with ablation of both alleles of the *Casr* gene in a C57/B6 background were generated by breeding the floxed-CaSR mice and the mice expressing Cre recombinase transgene under the control of a 2.3-kb promoter of rat type I collagen α-subunit as described previously (1). All mice were housed in a pathogen-free climate-controlled room (22 °C; 50% relative humidity) with a 12:/12-h dark/light cycle, given filtered water and standard chow containing 1.0% calcium and 0.7% phosphate, and euthanized at 3 months of age by isoflurane overdose for subsequent harvests of serum and bone samples. All animal procedures were approved by the Institutional Animal Care and Use Committee at the San Francisco Veterans Affairs Medical Center. Femurs and tibiae from WT and heterozygous and homozygous osteoblast-specific CaSR knockout mice (1) were used for immunofluorescent (IF) and Western blotting analyses of either CaSR, Homer1, or OPG. Femurs were snap-frozen and kept at −80 °C prior to protein extraction for Western blot analysis. Tibiae were cleaned, fixed in 10% formalin, decalcified, and sectioned at 8 μm-thick for IF. Sections were stained for IF as described below.

HEK-293 transient transfection—Cells were transiently transfected using the X-tremeGENE HP DNA transfection reagent (Roche Applied Science) under serum-free conditions and were used for subsequent experiments 48 h after transfection. The pRK5-Homer1c construct was the kind gift of Dr. RaoZhu Lin and Prof Paul Worley (Johns Hopkins School of Medicine).

siRNA transfection—Each siRNA used in this study was a commercially supplied (Santa Cruz Biotechnology) pool of three target-specific 19–25-nucleotide siRNAs designed to knock down expression of the specific gene of interest. siRNA sequences are listed in Table S1. siRNAs against all target transcripts were used at a concentration of 50 nM in the presence of siRNA transfection reagent (Santa Cruz Biotechnology) according to the manufacturer's instructions. Control transfections containing a nondirected siRNA sequence were carried out simultaneously, on the same plate, for all experiments. Briefly, osteoblasts were transfected overnight under serum-free conditions and permitted to grow for an additional 24 h in complete growth media after transfection, which allowed efficient reduction to the level of the targeted protein. Protein knockdown was confirmed by Western blotting.

Immunofluorescence (mouse bones)—Tibial sections were deparaffinized, cleared in xylene, rehydrated in ethanol steps, and permeabilized in Triton X-100 (0.5%). Bone sections were then blocked in 2% BSA for 30 min before being probed with anti-CaSR (goat polyclonal, clone F-19) or anti-Homer1 (rabbit polyclonal, clone H-174) followed by anti-goat Alexa Fluor 488 and anti-rabbit Cy3. To visualize the nuclei, coverslips were mounted with UltraCruz™ mounting medium containing 4′,6-diamidino-2-phenylindole (DAPI). Slides were observed under an Axio Imager 2 deconvolution microscope with Zeiss Apotome 2 imaging system (Zeiss, Oberkochen Germany) at the Advanced Microscopy Facility (Bosch Research Institute, University of Sydney).

Immunofluorescence (human osteoblasts)—Human osteoblasts were grown on poly-L-lysine–coated coverslips and were fixed with 4% (w/v) paraformaldehyde followed by 100% ice-cold methanol and were processed with the following antibodies: anti-CaSR (Sigma, mouse monoclonal, clone HL1499), anti-Homer1 (Santa Cruz Biotechnology, rabbit polyclonal, clone H-174), and isotype controls. Coverslips were then washed and incubated with anti-rabbit Alexa Fluor 488 (1:750; Santa Cruz Biotechnology) and anti-mouse Cy3 (1:750; Life Technologies, Inc.) at room temperature for 60 min. To visualize the nuclei, coverslips were mounted with UltraCruz™ mounting medium containing DAPI. Slides were observed under a LSM510 Meta confocal laser microscope (Zeiss) at the Advanced Microscopy Facility (Bosch Research Institute, University of Sydney).

Images for co-localization analysis were taken using the ×63 objective under oil. Background threshold levels were determined using ImageJ software (W. Rasband, National Institutes of Health), and Pearson's co-localization coefficients (47, 48) were calculated using the Coloc2 plugin of ImageJ.

Protein extraction from mouse bones—Following the removal of bone marrow, total protein was extracted from mouse bones using a combination of de-mineralization and chemical denaturation as described previously (49). Protein extracts were precipitated from their chemical denaturation solutions, and equal amounts of protein were subjected to Western blot analysis, and densitometry was carried out on triplicate bands.

Western blotting—For phosphoprotein detection, following inhibitor treatment or siRNA transfection, cells were permitted to equilibrate for 90 min in OptiMEM^{TM} (adjusted to contain a final concentration of 1 mM Ca^{2+}). The indicated concentration of Ca^{2+} (or the vehicle treatment) was then added to the cells for the indicated period (typically 15 min) prior to lysis. Following treatment, monolayer cultures were solubilized and analyzed by SDS-PAGE under reducing conditions followed by Western blotting to nitrocellulose membranes, as described previously (6). Primary antibodies for phosphoprotein detection were all from Cell Signaling Technology (CST) as follows: AKT–Ser^{473} (mouse monoclonal, clone 587F11); AKT–Ser^{473} (rabbit monoclonal, clone D9E); AKT–Thr^{308} (mouse monoclonal, clone L32A4); GSK3α/β–Ser$^{21/9}$ (rabbit polyclonal #9327); β-catenin–Ser^{552} (rabbit polyclonal #9566); and mTOR–Ser^{2448} (rabbit polyclonal #2971). Total (pan) protein detection antibodies were as follows: AKT (CST, mouse monoclonal, clone 40D4); GSK3β (CST, rabbit monoclonal, clone D5C5Z); β-catenin (Sigma, rabbit polyclonal #C2206); mTOR (CST, rabbit polyclonal, #2972); β-actin (Santa Cruz Biotechnology, mouse monoclonal, clone C4); GAPDH (CST, rabbit monoclonal, clone 14C10); CaSR (Sigma, mouse monoclonal, clone HL1499); Homer1 (Santa Cruz Biotechnology, mouse monoclonal, clone B5; rabbit polyclonal, #H-174); Gα12 (Santa Cruz Biotechnology, mouse monoclonal, clone E12); Raptor (CST, rabbit monoclonal, clone 24C12); Rictor (CST, rabbit monoclonal, clone D16H9); OPG (R&D Systems, biotinylated goat polyclonal #BAF805); laminB1 (Thermo Fisher Scientific, mouse monoclonal, clone L5).

Alkaline phosphatase activity—Following treatment, human osteoblasts in triplicate wells of 96-well plates were lysed in PBS containing 0.1% (v/v) Triton X-100. An equal volume of 0.2 M glycine (pH 9.5) containing 1 mg/ml 4-pNPP (ALP substrate) was added to start the enzymatic reaction. The reaction was simultaneously carried out with calf intestinal ALP (0–1 unit) under the same conditions to construct a standard curve. Identically treated wells on the same plate were used for cell number correction determined by total cellular protein (BCA).

Caspase-3 activity—Following treatment, apoptosis was assessed in human osteoblasts in triplicate wells of 96-well plates via caspase-3 activity with the peptide substrate Ac-DEVD-AFC (BD Biosciences) used according to the manufacturer's instructions. Identically treated wells on the same plate were used for cell number correction determined by total cellular protein (BCA).

Nuclear localization of β-catenin—Detection of β-catenin localized to the nucleus was performed as described previously (6). Briefly, following treatment, osteoblast monolayers were lysed in 10 mM Tris (pH 7.5), 10 mM NaCl, 3 mM $MgCl_2$, 0.5% (v/v) Nonidet P-40, with protease inhibitors for 5 min on ice. Lysates were centrifuged at 500 × *g* for 30 min at 4 °C, and the pellet washed three times with lysis buffer. Insoluble pellet was resuspended in a high salt buffer (10 mM Tris (pH 7.5), 0.4 M NaCl for 30 min on ice, centrifuged at 12,000 × *g* for 30 min at 4 °C, and the resulting supernatant represented the nuclear fraction. Protein concentrations were normalized between treatments (BCA), and equal amounts of protein were subjected to Western blot analysis. LaminB1 was used as a loading control for the nuclear fraction.

Co-immunoprecipitation—Human osteoblasts in triplicate wells of 6-well plates were exposed to control (1.0 mM) or elevated (3.5 mM) Ca^{2+} concentration for 2 min, immunoprecipitated with anti-Homer-1–b/c using a variation of a protocol previously described (50). Briefly, following treatment, the cell monolayer was lysed on ice in 50 mM Tris (pH 7.5), 250 mM NaCl, 1% (v/v) Nonidet P-40 with protease inhibitors, and lysates from triplicate wells were combined and processed through a 21-gauge needle five times. Insoluble material was removed by centrifugation, and the lysate was pre-cleared with protein-A/G PLUS–agarose beads (20 μl/ml). Following protein concentration measurement, immunoprecipitation of 1 mg of total cellular lysate with 1 μg/ml monoclonal anti-Homer1 (Santa Cruz Biotechnology, rabbit polyclonal, #H-174) (or isotype control) was carried out overnight at 4 °C with protein-A/G PLUS–agarose (20 μl/ml) with orbital mixing. Beads were extensively washed in lysis buffer prior to detection of immunoprecipitated protein by Western blotting under reducing conditions using VeriBlot^{TM} secondary antibodies (Abcam). As with other Western blottings, this experiment was performed three times for quantification.

OPG protein—OPG protein levels *in vitro* were detected by whole-cell ELISA. OPG protein levels in the supernatant of primary osteoblasts were routinely at the lower limit of detection by capture ELISA, but the protein was readily found to be associated with the cell monolayer. For this reason, a whole-cell ELISA was developed. Following treatment, cells were fixed with 10% neutral buffered formalin for 5 min and then permeabilized with three incubations with PBS, 0.1% (v/v) Triton X-100 for 5 min each. Endogenous peroxidase was inactivated with 0.6% H_2O_2 in PBS for 15 min. Wells were blocked with 5% (w/v) BSA in PBS for 30 min. Detection was with anti-OPG mAb (mouse monoclonal, clone #69127, R&D Systems) or an isotype control for background correction, in blocker at 4 °C on a rocking platform overnight followed by anti-Ig–horseradish peroxidase conjugated at 1 μg/ml in blocker for 1 h at room temperature and subsequent 3,3′,5,5′-tetramethylbenzidine detection. All steps were separated by five PBS, 0.01% (v/v) Tween 20 washes.

qPCR protocol for Wnt SuperArray—We used the reverse transcription (RT^2) Profiler PCR Array Mouse Wnt signaling pathway array purchased from SuperArray Bioscience (Frederick, MD). The complete gene list is available online. Total RNA from marrow-flushed mouse bones was isolated using the RNA Stat-60 (Amsbio, Cambridge, MA). First-strand cDNA synthesis reaction was performed as follows: 2 μg of extracted RNA was mixed with 10 μl of the SuperArray RT mixture mix. The products were then incubated at 37 °C for 1 h and heated at 95 °C for 5 min. Real-time–based SYBR Green PCR was performed using a ViiA7 real-time PCR system (Thermo Fisher

Scientific), and the following thermal cycling condition was used: 95 °C for 10 min, followed by 40 cycles of 95 °C for 15 s and 60 °C for 60 s. Data analysis and the cycle threshold (*CT*) values, which were defined as the fractional cycle number at which the fluorescence passes an arbitrarily set threshold, were analyzed using the built-in ViiA7 analytic software. The *CT* value of each gene was normalized to that of *ACTB*, which is included in this commercially available kit.

CellTiter-Blue®—The cell viability dye CellTiter-Blue® (Promega) was used according to the manufacturer's instruction. Fluorescence of the dye was measured at $\lambda Ex_{560}/\lambda Em_{590}$.

Statistics and data analysis—Experiments were performed in triplicate. Each experiment was repeated at least three times, with cells from different donors, and the data are reported as means ± S.D. One-way analysis of variance with the Tukey post-test were used to determine significant differences between treatments using Prism (GraphPad Software Inc).

Author contributions—M. S. R., R. S. M., and A. D. C. conceptualization; M. S. R. and K. S. I. data curation; M. S. R., K. S. I., and T. C. B.-S. formal analysis; M. S. R. validation; M. S. R., K. S. I., T. C. B.-S., Z. C., S. C. B., W. C., R. S. M., and A. D. C. investigation; M. S. R., R. S. M., and A. D. C. visualization; M. S. R., K. S. I., T. C. B.-S., Z. C., and W. C. methodology; M. S. R., R. S. M., and A. D. C. writing-original draft; M. S. R., R. S. M., and A. D. C. project administration; M. S. R., T. C. B.-S., W. C., R. S. M., and A. D. C. writing-review and editing; Z. C., W. C., R. S. M., and A. D. C. resources; R. S. M. and A. D. C. supervision; R. S. M. and A. D. C. funding acquisition.

References

1. Chang, W., Tu, C., Chen, T. H., Bikle, D., and Shoback, D. (2008) The extracellular calcium-sensing receptor (CaSR) is a critical modulator of skeletal development. *Sci. Signal.* **1,** ra1 CrossRef Medline
2. Dvorak-Ewell, M. M., Chen, T. H., Liang, N., Garvey, C., Liu, B., Tu, C., Chang, W., Bikle, D. D., and Shoback, D. M. (2011) Osteoblast extracellular Ca^{2+}-sensing receptor regulates bone development, mineralization, and turnover. *J. Bone Miner. Res.* **26,** 2935–2947 CrossRef Medline
3. Goltzman, D., and Hendy, G. N. (2015) The calcium-sensing receptor in bone–mechanistic and therapeutic insights. *Nat. Rev. Endocrinol.* **11,** 298–307 CrossRef Medline
4. Ruat, M., and Traiffort, E. (2013) Roles of the calcium sensing receptor in the central nervous system. *Best Pract. Res. Clin. Endocrinol. Metab.* **27,** 429–442 CrossRef Medline
5. Ward, B. K., Magno, A. L., Davis, E. A., Hanyaloglu, A. C., Stuckey, B. G., Burrows, M., Eidne, K. A., Charles, A. K., and Ratajczak, T. (2004) Functional deletion of the calcium-sensing receptor in a case of neonatal severe hyperparathyroidism. *J. Clin. Endocrinol. Metab.* **89,** 3721–3730 CrossRef Medline
6. Rybchyn, M. S., Slater, M., Conigrave, A. D., and Mason, R. S. (2011) An Akt-dependent increase in canonical Wnt signaling and a decrease in sclerostin protein levels are involved in strontium ranelate-induced osteogenic effects in human osteoblasts. *J. Biol. Chem.* **286,** 23771–23779 CrossRef Medline
7. Burgering, B. M., and Coffer, P. J. (1995) Protein kinase B (c-Akt) in phosphatidylinositol-3-OH kinase signal transduction. *Nature* **376,** 599–602 CrossRef Medline
8. Franke, T. F., Yang, S. I., Chan, T. O., Datta, K., Kazlauskas, A., Morrison, D. K., Kaplan, D. R., and Tsichlis, P. N. (1995) The protein kinase encoded by the Akt proto-oncogene is a target of the PDGF-activated phosphatidylinositol 3-kinase. *Cell* **81,** 727–736 CrossRef Medline
9. Sarbassov, D. D., Guertin, D. A., Ali, S. M., and Sabatini, D. M. (2005) Phosphorylation and regulation of Akt/PKB by the rictor–mTOR complex. *Science* **307,** 1098–1101 CrossRef Medline
10. Jacinto, E., Facchinetti, V., Liu, D., Soto, N., Wei, S., Jung, S. Y., Huang, Q., Qin, J., and Su, B. (2006) SIN1/MIP1 maintains rictor–mTOR complex integrity and regulates Akt phosphorylation and substrate specificity. *Cell* **127,** 125–137 CrossRef Medline
11. Guertin, D. A., Stevens, D. M., Thoreen, C. C., Burds, A. A., Kalaany, N. Y., Moffat, J., Brown, M., Fitzgerald, K. J., and Sabatini, D. M. (2006) Ablation in mice of the mTORC components raptor, rictor, or mLST8 reveals that mTORC2 is required for signaling to Akt-FOXO and PKCα, but not S6K1. *Dev. Cell* **11,** 859–871 CrossRef Medline
12. Sarbassov, D. D., Ali, S. M., Kim, D. H., Guertin, D. A., Latek, R. R., Erdjument-Bromage, H., Tempst, P., and Sabatini, D. M. (2004) Rictor, a novel binding partner of mTOR, defines a rapamycin-insensitive and raptor-independent pathway that regulates the cytoskeleton. *Curr. Biol.* **14,** 1296–1302 CrossRef Medline
13. Ebner, M., Sinkovics, B., Szczygiel, M., Ribeiro, D. W., and Yudushkin, I. (2017) Localization of mTORC2 activity inside cells. *J. Cell Biol.* **216,** 343–353 CrossRef Medline
14. Kubota, T., Michigami, T., and Ozono, K. (2009) Wnt signaling in bone metabolism. *J. Bone Miner. Metab.* **27,** 265–271 CrossRef Medline
15. Baron, R., and Kneissel, M. (2013) WNT signaling in bone homeostasis and disease: from human mutations to treatments. *Nat. Med.* **19,** 179–192 CrossRef Medline
16. Clevers, H. (2006) Wnt/β-catenin signaling in development and disease. *Cell* **127,** 469–480 CrossRef Medline
17. Srivastava, A. K., and Pandey, S. K. (1998) Potential mechanism(s) involved in the regulation of glycogen synthesis by insulin. *Mol. Cell. Biochem.* **182,** 135–141 CrossRef Medline
18. Cross, D. A., Alessi, D. R., Cohen, P., Andjelkovich, M., and Hemmings, B. A. (1995) Inhibition of glycogen synthase kinase-3 by insulin mediated by protein kinase B. *Nature* **378,** 785–789 CrossRef Medline
19. Fang, D., Hawke, D., Zheng, Y., Xia, Y., Meisenhelder, J., Nika, H., Mills, G. B., Kobayashi, R., Hunter, T., and Lu, Z. (2007) Phosphorylation of β-catenin by AKT promotes β-catenin transcriptional activity. *J. Biol. Chem.* **282,** 11221–11229 CrossRef Medline
20. Esen, E., Chen, J., Karner, C. M., Okunade, A. L., Patterson, B. W., and Long, F. (2013) WNT-LRP5 signaling induces Warburg effect through mTORC2 activation during osteoblast differentiation. *Cell Metab.* **17,** 745–755 CrossRef Medline
21. Brakeman, P. R., Lanahan, A. A., O'Brien, R., Roche, K., Barnes, C. A., Huganir, R. L., and Worley, P. F. (1997) Homer: a protein that selectively binds metabotropic glutamate receptors. *Nature* **386,** 284–288 CrossRef Medline
22. Rong, R., Ahn, J. Y., Huang, H., Nagata, E., Kalman, D., Kapp, J. A., Tu, J., Worley, P. F., Snyder, S. H., and Ye, K. (2003) PI3 kinase enhancer–Homer complex couples mGluRI to PI3 kinase, preventing neuronal apoptosis. *Nat. Neurosci.* **6,** 1153–1161 CrossRef Medline
23. Mao, L., Yang, L., Tang, Q., Samdani, S., Zhang, G., and Wang, J. Q. (2005) The scaffold protein Homer1b/c links metabotropic glutamate receptor 5 to extracellular signal-regulated protein kinase cascades in neurons. *J. Neurosci.* **25,** 2741–2752 CrossRef Medline
24. Ronesi, J. A., and Huber, K. M. (2008) Homer interactions are necessary for metabotropic glutamate receptor-induced long-term depression and translational activation. *J. Neurosci.* **28,** 543–547 CrossRef Medline
25. Xiao, B., Tu, J. C., Petralia, R. S., Yuan, J. P., Doan, A., Breder, C. D., Ruggiero, A., Lanahan, A. A., Wenthold, R. J., and Worley, P. F. (1998) Homer regulates the association of group 1 metabotropic glutamate receptors with multivalent complexes of homer-related, synaptic proteins. *Neuron* **21,** 707–716 CrossRef Medline
26. Bockaert, J., Perroy, J., Bécamel, C., Marin, P., and Fagni, L. (2010) GPCR interacting proteins (GIPs) in the nervous system: roles in physiology and pathologies. *Annu. Rev. Pharmacol. Toxicol.* **50,** 89–109 CrossRef Medline
27. Shiraishi-Yamaguchi, Y., and Furuichi, T. (2007) The Homer family proteins. *Genome Biol.* **8,** 206 CrossRef Medline

28. Ranganathan, R., and Ross, E. M. (1997) PDZ domain proteins: scaffolds for signaling complexes. *Curr. Biol.* **7,** R770–R773 CrossRef Medline
29. Worley, P. F., Zeng, W., Huang, G., Kim, J. Y., Shin, D. M., Kim, M. S., Yuan, J. P., Kiselyov, K., and Muallem, S. (2007) Homer proteins in Ca^{2+} signaling by excitable and non-excitable cells. *Cell Calcium* **42,** 363–371 CrossRef Medline
30. Chiang, G. G., and Abraham, R. T. (2005) Phosphorylation of mammalian target of rapamycin (mTOR) at Ser-2448 is mediated by p70S6 kinase. *J. Biol. Chem.* **280,** 25485–25490 CrossRef Medline
31. O'Reilly, K. E., Rojo, F., She, Q. B., Solit, D., Mills, G. B., Smith, D., Lane, H., Hofmann, F., Hicklin, D. J., Ludwig, D. L., Baselga, J., and Rosen, N. (2006) mTOR inhibition induces upstream receptor tyrosine kinase signaling and activates Akt. *Cancer Res.* **66,** 1500–1508 CrossRef Medline
32. Sun, S. Y., Rosenberg, L. M., Wang, X., Zhou, Z., Yue, P., Fu, H., and Khuri, F. R. (2005) Activation of Akt and eIF4E survival pathways by rapamycin-mediated mammalian target of rapamycin inhibition. *Cancer Res.* **65,** 7052–7058 CrossRef Medline
33. Bai, M., Trivedi, S., and Brown, E. M. (1998) Dimerization of the extracellular calcium-sensing receptor (CaR) on the cell surface of CaR-transfected HEK293 cells. *J. Biol. Chem.* **273,** 23605–23610 CrossRef Medline
34. Voyno-Yasenetskaya, T. A., Faure, M. P., Ahn, N. G., and Bourne, H. R. (1996) Gα12 and Gα13 regulate extracellular signal-regulated kinase and c-Jun kinase pathways by different mechanisms in COS-7 cells. *J. Biol. Chem.* **271,** 21081–21087 CrossRef Medline
35. Wang, J., and Stern, P. H. (2010) Osteoclastogenic activity and RANKL expression are inhibited in osteoblastic cells expressing constitutively active Gα(12) or constitutively active RhoA. *J. Cell. Biochem.* **111,** 1531–1536 CrossRef Medline
36. Rawadi, G., Vayssière, B., Dunn, F., Baron, R., and Roman-Roman, S. (2003) BMP-2 controls alkaline phosphatase expression and osteoblast mineralization by a Wnt autocrine loop. *J. Bone Miner. Res.* **18,** 1842–1853 CrossRef Medline
37. Manolagas, S. C. (2010) From estrogen-centric to aging and oxidative stress: a revised perspective of the pathogenesis of osteoporosis. *Endocr. Rev.* **31,** 266–300 CrossRef Medline
38. Conigrave, A. D., Quinn, S. J., and Brown, E. M. (2000) L-Amino acid sensing by the extracellular Ca^{2+}-sensing receptor. *Proc. Natl. Acad. Sci. U.S.A.* **97,** 4814–4819 CrossRef Medline
39. McCormick, W. D., Atkinson-Dell, R., Campion, K. L., Mun, H. C., Conigrave, A. D., and Ward, D. T. (2010) Increased receptor stimulation elicits differential calcium-sensing receptor(T888) dephosphorylation. *J. Biol. Chem.* **285,** 14170–14177 CrossRef Medline
40. Xiao, B., Tu, J. C., and Worley, P. F. (2000) Homer: a link between neural activity and glutamate receptor function. *Curr. Opin. Neurobiol.* **10,** 370–374 CrossRef Medline
41. Manolagas, S. C., and Parfitt, A. M. (2010) What old means to bone. *Trends Endocrinol. Metab.* **21,** 369–374 CrossRef Medline
42. Khanna, N., Fang, Y., Yoon, M. S., and Chen, J. (2013) XPLN is an endogenous inhibitor of mTORC2. *Proc. Natl. Acad. Sci. U.S.A.* **110,** 15979–15984 CrossRef Medline
43. Avila-Flores, A., Santos, T., Rincón, E., and Mérida, I. (2005) Modulation of the mammalian target of rapamycin pathway by diacylglycerol kinase-produced phosphatidic acid. *J. Biol. Chem.* **280,** 10091–10099 CrossRef Medline
44. Slater, M., Patava, J., and Mason, R. S. (1994) Role of chondroitin sulfate glycosaminoglycans in mineralizing osteoblast-like cells: effects of hormonal manipulation. *J. Bone Miner. Res.* **9,** 161–169 CrossRef Medline
45. Brennan, T. C., Rybchyn, M. S., Green, W., Atwa, S., Conigrave, A. D., and Mason, R. S. (2009) Osteoblasts play key roles in the mechanisms of action of strontium ranelate. *Br. J. Pharmacol.* **157,** 1291–1300 CrossRef Medline
46. Levinger, I., Seeman, E., Jerums, G., McConell, G. K., Rybchyn, M. S., Cassar, S., Byrnes, E., Selig, S., Mason, R. S., Ebeling, P. R., and Brennan-Speranza, T. C. (2016) Glucose-loading reduces bone remodeling in women and osteoblast function *in vitro*. *Physiol. Rep.* **4,** e12700 CrossRef
47. Dunn, K. W., Kamocka, M. M., and McDonald, J. H. (2011) A practical guide to evaluating co-localization in biological microscopy. *Am. J. Physiol. Cell Physiol.* **300,** C723–C742 CrossRef Medline
48. Manders, E. M., Verbeek, F. J., and Aten, J. A. (1993) Measurement of co-localization of objects in dual-color confocal images. *J. Microsc.* **169,** 375–382 CrossRef
49. Jiang, X., Ye, M., Jiang, X., Liu, G., Feng, S., Cui, L., and Zou, H. (2007) Method development of efficient protein extraction in bone tissue for proteome analysis. *J. Proteome Res.* **6,** 2287–2294 CrossRef Medline
50. Sequeira, V. B., Rybchyn, M. S., Tongkao-On, W., Gordon-Thomson, C., Malloy, P. J., Nemere, I., Norman, A. W., Reeve, V. E., Halliday, G. M., Feldman, D., and Mason, R. S. (2012) The role of the vitamin D receptor and ERp57 in photoprotection by 1α,25-dihydroxyvitamin D3. *Mol. Endocrinol.* **26,** 574–582 CrossRef Medline